

# Myocardial triglycerides in cardiac amyloidosis assessed by proton cardiovascular magnetic resonance spectroscopy

**Journal Article****Author(s):**

Gastl, Mareike; Peereboom, Sophie M.; Gotschy, Alexander; Fuetterer, Maximilian; Deuster, von Deuster, Constantin; Boenner, Florian; Kelm, Malte; Schwotzer, Rahel; Flammer, Andreas J.; Manka, Robert; Kozerke, Sebastian

**Publication date:**

2019

**Permanent link:**

<https://doi.org/10.3929/ethz-b-000323988>

**Rights / license:**

[Creative Commons Attribution 4.0 International](#)

**Originally published in:**


Journal of Cardiovascular Magnetic Resonance 21(1), <https://doi.org/10.1186/s12968-019-0519-6>

RESEARCH

Open Access



# Myocardial triglycerides in cardiac amyloidosis assessed by proton cardiovascular magnetic resonance spectroscopy

Mareike Gastl<sup>1,2,3\*</sup> , Sophie M. Peereboom<sup>1</sup>, Alexander Gotschy<sup>1,2</sup>, Maximilian Fuetterer<sup>1</sup>, Constantin von Deuster<sup>1</sup>, Florian Boenner<sup>3</sup>, Malte Kelm<sup>3</sup>, Rahel Schwotzer<sup>4</sup>, Andreas J. Flammer<sup>2</sup>, Robert Manka<sup>1,2,5</sup> and Sebastian Kozerke<sup>1</sup>

## Abstract

**Background:** Cardiac involvement of amyloidosis leads to left-ventricular (LV) wall thickening with progressive heart failure requiring rehospitalization. Cardiovascular magnetic resonance (CMR) is a valuable tool to non-invasively assess myocardial thickening as well as structural changes. Proton CMR spectroscopy (<sup>1</sup>H-CMRS) additionally allows assessing metabolites including triglycerides (TG) and total creatine (CR). However, opposing results exist regarding utilization of these metabolites in LV hypertrophy or thickening. Therefore, the aim of this study was to measure metabolic alterations using <sup>1</sup>H-CMRS in a group of patients with thickened myocardium caused by cardiac amyloidosis.

**Methods:** <sup>1</sup>H-CMRS was performed on a 1.5 T system (Achieva, Philips Healthcare, Best, The Netherlands) using a 5-channel receive coil in 11 patients with cardiac amyloidosis (60.5 ± 11.4 years, 8 males) and 11 age- and gender-matched controls (63.2 ± 8.9 years, 8 males). After cardiac morphology and function assessment, proton spectra from the interventricular septum (IVS) were acquired using a double-triggered PRESS sequence. Post-processing was performed using a customized reconstruction pipeline based on ReconFrame (GyroTools LLC, Zurich, Switzerland). Spectra were fitted in jMRUI/AMARES and the ratios of triglyceride-to-water (TG/W) and total creatine-to-water (CR/W) were calculated.

**Results:** Besides an increased LV mass and a thickened IVS concomitant to the disease characteristics, patients with cardiac amyloidosis presented with decreased global longitudinal (GLS) and circumferential (GCS) strain. LV ejection fraction was preserved relative to controls (60.0 ± 13.2 vs. 66.1 ± 4.3%, *p* = 0.17). Myocardial TG/W ratios were significantly decreased compared to controls (0.53 ± 0.23 vs. 0.80 ± 0.26%, *p* = 0.015). CR/W ratios did not show a difference between both groups, but a higher standard deviation in patients with cardiac amyloidosis was observed. Pearson correlation revealed a negative association between elevated LV mass and TG/W (*R* = -0.59, *p* = 0.004) as well as GCS (*R* = -0.48, *p* = 0.025).

**Conclusions:** A decrease in myocardial TG/W can be detected in patients with cardiac amyloidosis alongside impaired cardiac function with an association to the degree of myocardial thickening. Accordingly, <sup>1</sup>H-CMRS may provide an additional diagnostic tool to gauge progression of cardiac amyloidosis along with standard imaging sequences.

(Continued on next page)

\* Correspondence: [gastl@biomed.ee.ethz.ch](mailto:gastl@biomed.ee.ethz.ch)

<sup>1</sup>Institute for Biomedical Engineering, University and ETH Zurich, Gloriastrasse 35, 8092 Zurich, Switzerland

<sup>2</sup>Department of Cardiology, University Heart Center, University Hospital Zurich, Zurich, Switzerland

Full list of author information is available at the end of the article



(Continued from previous page)

**Trial registration:** EK 2013–0132.

**Keywords:** Cardiac amyloidosis, Cardiovascular magnetic resonance, Proton spectroscopy, Myocardial metabolism, Left-ventricular thickening

## Background

Amyloidosis is a multisystemic disorder which is characterized by extracellular deposition of misfolded amyloid proteins leading to consecutive organ failure [1]. Cardiac involvement is frequent. The most common types are acquired or inherited transthyretin-related (ATTR) and light-chain (AL) amyloidosis. Once affected, prognosis and outcome of patients with cardiac amyloidosis deteriorates dependent on the subtype, hence requiring sufficient diagnostic accuracy and follow-up strategies [2, 3]. Currently, definite diagnosis of cardiac amyloidosis is established using either invasive tissue biopsy for all types or technetium scintigraphy in ATTR amyloidosis respectively [4, 5]. Cardiovascular magnetic resonance (CMR) is increasingly used for screening purposes in patients with suspected cardiac involvement of amyloidosis due to its non-invasive nature and its potential to characterize different forms of amyloidosis [6, 7]. Typical cardiac manifestations include myocardial thickening and diffuse late gadolinium enhancement (LGE) resulting from expanded extracellular space. However, the expression of cardiac amyloidosis and its sub-forms can be heterogeneous and the differentiation from other forms of myocardial thickening may be challenging at early stages [1]. Besides the detection of morphological and structural changes with CMR, proton spectroscopy may offer additional insights into the metabolism of healthy and diseased hearts [8, 9]. In particular, myocardial triglyceride (TG) and total creatine (CR) content can be determined [9].

In the healthy human heart,  $\beta$ -oxidation of fatty acids constitutes the major mechanism of energy production that is subject to storage of TG [10]. In thickened hearts, mainly in left-ventricular (LV) hypertrophy (LVH), studies have provided controversial results about TG utilization. In particular, myocardial TG was found to be significantly reduced in hypertrophic cardiomyopathy (HCM) while no changes were found in LVH associated with Anderson-Fabry's disease [11–13]. Potential metabolic alterations involved in myocardial thickening due to cardiac amyloidosis have not been studied in detail and previous histological and proton spectroscopy studies present with contradictory results. On the one hand, reduced TG utilization has been found to associate with advanced stages of heart failure and HCM while, on the other hand, histopathological analyses revealed an association of fatty acids with amyloid proteins [8, 14, 15].

Therefore, the objective of the present study was to assess myocardial TG and additional CR content along with functional parameters in a group of patients with cardiac amyloidosis using CMR imaging and spectroscopy.

## Methods

The study was conducted in accordance to the declaration of Helsinki and its later amendments. Local ethics committee approval was obtained. All data acquired in this study were handled anonymously and written informed consent was obtained from each subject.

### Study population

Eleven patients with cardiac amyloidosis ( $60.5 \pm 11.4$  years, 8 males, AL = 7, ATTR = 4) were recruited from the interdisciplinary “Amyloidosis-Network” of the University Hospital Zurich. Cardiac involvement of systemic amyloidosis was confirmed by endomyocardial biopsy, biopsy of other tissue (fat, lips) or by imaging [4, 16]. Amyloidosis patients as well as 11 age- and gender matched controls ( $63.2 \pm 8.9$  years, 8 males) received CMR imaging and spectroscopy at the University Hospital Zurich, Switzerland. In addition, blood lipid- and N-terminal pro-hormone of brain natriuretic peptide-levels (NT-proBNP) were measured by acquiring blood samples. Subjects were advised to adhere to a 3-h fasting period prior to the CMR examination and scans were performed at afternoon times.

### Data acquisition

CMR imaging and spectroscopy was performed on a 1.5 T system (Achieva, Philips Healthcare, Best, The Netherlands) using a 5-channel phased array coil. After scout and reference scans, anatomical and geometric data were acquired using balanced steady-state free precession (bSSFP) sequence in standard long-axis geometries (two-, three- and four-chamber view) as well as in short-axis view with full LV coverage from base to apex (repetition time (TR)/echo time (TE) = 3.3 / 1.6 ms, flip angle = 60°, spatial resolution =  $1.5 \times 1.5 \times 8$  mm<sup>3</sup>, 50 phases, 2 slices per breathhold).

In cases with an estimated glomerular filtration rate (eGFR) > 35 mL/min and informed consent of the subject, a gadolinium-based contrast agent (Gadovist, Bayer Healthcare, Berlin, Germany) was injected for LGE imaging to visualize fibrosis and scarring. Ethical approval constrains only allowed the administration of

contrast agent in amyloidosis patients. All patients were eligible to receive gadolinium. After a period of 10 min, a 3-dimensional gradient spoiled turbo fast-field echo sequence with a non-selective  $180^\circ$  inversion pre-pulse was performed at end diastole (TR/TE = 3.3/1.6 ms, flip angle =  $15^\circ$ , spatial resolution =  $1.6 \times 1.6 \times 5 \text{ mm}^3$ , adjusted inversion delay, one breath-hold for each anatomical location) in the same anatomical location as the bSSFP scans [17].

### Spectroscopy

Spectroscopy data were acquired after anatomical cine imaging and prior to contrast agent injection. Cine imaging in four-chamber and short-axis views were repeated with navigator gating on the diaphragm for subsequent planning of the spectroscopic voxel and to account for potential subject movement during the scan session. Prior to the acquisition of spectroscopy data, iterative volume shimming was performed over a volume of  $15 \times 25 \times 45 \text{ mm}^3$  during a single breathhold. Thereafter, voxels of 7–8 mL ( $10 \times 20 \times 35\text{--}40 \text{ mm}^3$ ) were positioned in the interventricular septum (IVS) and proton spectra were recorded using a PRESS (point-resolved spectroscopy) sequence in systole with optimized spoilers (Fig. 1) [18]. Spectroscopic data acquisition was double-triggered using electrocardiogram (ECG) triggering and pencil beam navigator-based respiratory gating on the diaphragm with a gating window of 4 mm. Water suppression was achieved by chemical shift selective saturation (CHESS) (excitation bandwidth 100 Hz) [19]. A total of 96 averages with water suppression and 16 averages without water suppression were recorded at a spectral bandwidth of 2000 Hz (1024 samples) and a minimum TR of 2000 ms (TE = 22 ms, flip angle =  $90^\circ$ ).

### Post-processing

Functional and geometric parameter assessment based on imaging data was achieved using commercial post-processing software (IntelliSpace Portal, Philips, Best, The Netherlands). The bSSFP imaging data were used to measure the IVS at maximum extension in end diastole, LV and right ventricular (RV) end-diastolic volume (LVEDV/RVEDV), left ventricular end-diastolic diameter (LVEDD), left and right ventricular ejection fraction (LVEF/RVEF), stroke volume (SV), and LVM indexed to body surface area (LVMI).

LV strain and strain rate analysis was performed using feature tracking analysis (Image-Arena VA Version 4.6 and 2D Cardiac Performance Analysis MR Version 4, TomTec Imaging Systems, Unterschleißheim, Germany). The bSSFP images were used to manually draw endocardial contours followed by software-driven automatic tracking. End-systolic global longitudinal (GLS) and circumferential strain (GCS) as well as peak diastolic longitudinal and circumferential strain rate were extracted.

Spectroscopy data were first reconstructed in MATLAB (The Mathworks, Natick, Massachusetts, USA) using a customized reconstruction pipeline based on ReconFrame (GyroTools LLC, Zurich, Switzerland) as illustrated in Fig. 2. After noise decorrelation, a singular value decomposition approach (SVD) was used for the combination of all five individual coil channels. Weights estimated from the water spectra were used for the calculation of water-unsuppressed and water-suppressed signals [20, 21]. Following this step, individual averages were phase-corrected. For non-water suppressed spectra, phasing was based on the water peak whereas for water-suppressed spectra, phasing was based on the peak

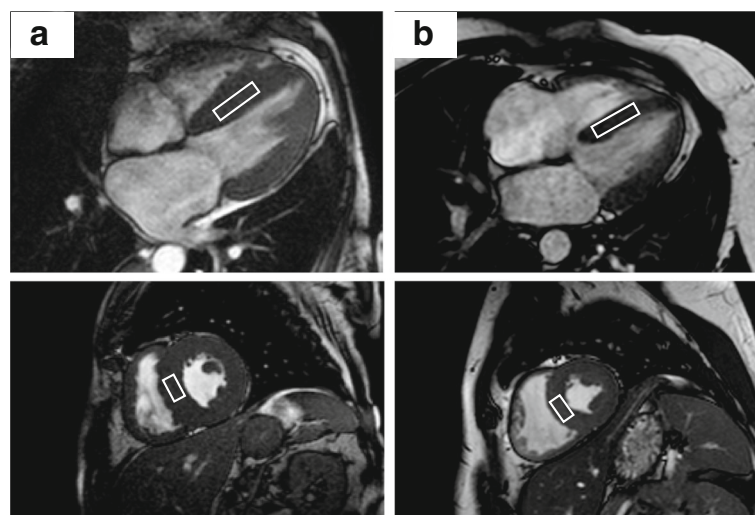
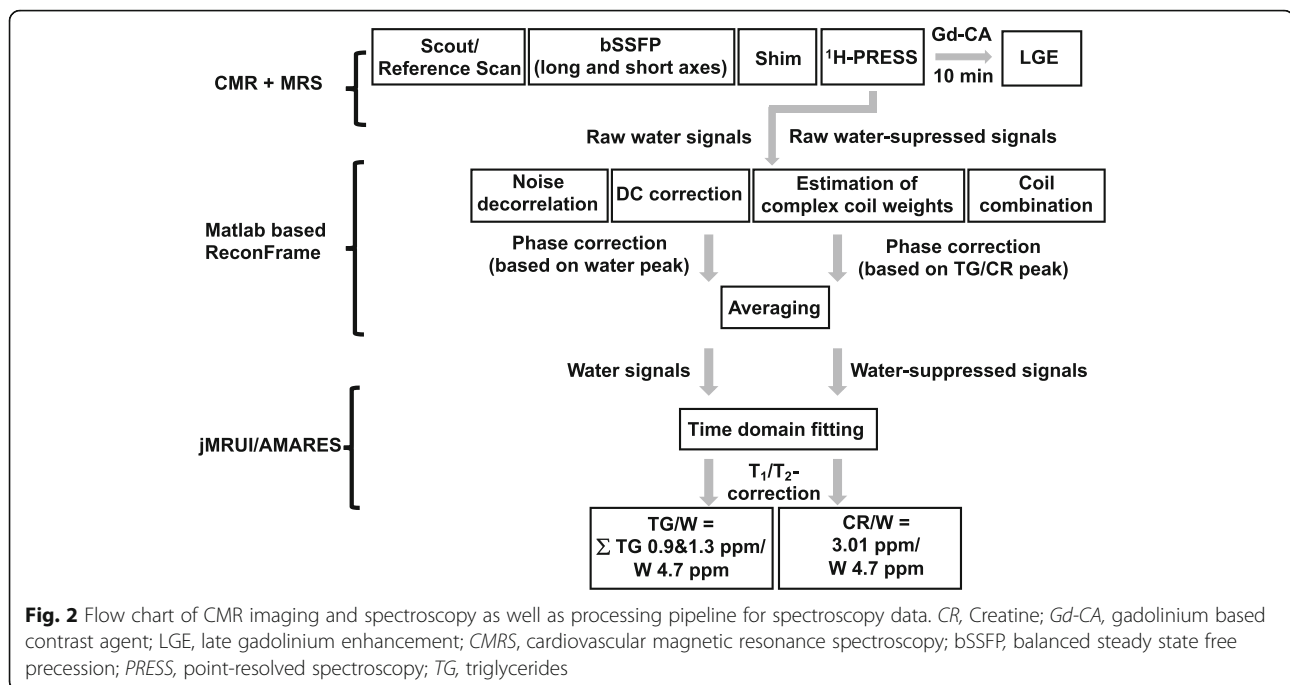


**Fig. 1** Position of the  $^1\text{H}$ -CMRS voxel within the IVS of a patient with cardiac amyloidosis (a) and of a normal control (b). IVS, interventricular septum;  $^1\text{H}$ -CMRS, Proton CMR spectroscopy



at 1.3 ppm for TG and on the peak at 3.01 ppm for CR. Afterwards, averaging was conducted.

Reconstructed and averaged spectra were analysed in jMRUI/AMARES (version 5.2) [22]. Water-unsuppressed and water-suppressed spectra were time-domain fitted using Lorentzian line shapes after first-order phase correction. A Hankel-Lanczos Singular Value Decomposition (HLSVD) approach was used to filter out the residual water peak and a total of six resonances were fitted to the water-suppressed spectra: (1) TG at 0.9, 1.3 and 2.1 ppm, (2) CR at 3.01 ppm, (3) trimethylammonium (TMA) at 3.2 ppm and (4) the residual water at 4.7 ppm. The maximum linewidth of all resonances was limited by soft constraints to 0.75 ppm and relative chemical shifts were used as fixed boundary conditions.

For the calculation of triglyceride- and creatine-to-water ratios (TG/W and CR/W), data were first corrected for longitudinal and transverse relaxation by using  $T_1 = 970$  ms and  $T_2 = 40$  ms for myocardial water,  $T_1 = 280$  ms and  $T_2 = 80$  ms for myocardial TG, and  $T_1 = 1480$  ms and  $T_2 = 135$  ms for CR [21, 23]. The TG/W ratio was then calculated as the sum of the fitted TG resonances at 0.9 and 1.3 ppm divided by the fitted water. The CR/W ratio was calculated from the CR resonance at 3.01 ppm divided by the fitted water signal.

The amount of fibrosis as percentage of LVMi was calculated semi-automatically by manually applying epi- and endocardial contours to the short-axis LGE images for every slice. Then, the amount of fibrosis was calculated using a full-width-at-half-maximum (FWHM) approach as previously described [24].

## Statistical analysis

Statistical analyses were conducted using SPSS (version 24.0, International Business Machines, Armonk, New York, US). Continuous variables are expressed as mean  $\pm$  standard deviation (SD). Categorical variables are reported as percentages. After testing for normal distribution using a Kolmogorov-Smirnov test, data between groups were compared using a 2-sided unpaired Student's t-test for normally distributed data and a non-parametric Mann-Whitney *U*-tests for not normally distributed data. Fisher's exact t-test was used to examine significant differences between nominal classifications. Bivariate Pearson correlation analysis was conducted to analyze relationships between different CMR parameter including <sup>1</sup>H-CMRS results. *P*-values below 0.05 were considered as statistically significant.

## Results

### Study population and clinical characteristics

Cardiovascular comorbidities, age- and sex were not significantly different between amyloidosis patients and the control group. Biochemical analyses revealed no differences in blood lipid levels between the groups (Table 1). NT-proBNP of amyloidosis patients was elevated according to recent heart failure guidelines [25].

### Imaging

Baseline CMR parameters of amyloidosis patients and controls are summarized in Table 2. Amyloidosis patients showed significantly elevated IVS and LVMi. LVEF as one surrogate for myocardial systolic function did not

**Table 1** Demographic and clinical baseline characteristics

	Amyloidosis (n = 11)	Controls (n = 11)	P-value
Age (years)	60.5 ± 11.4	62.9 ± 8.9	0.57
Male (%)	8 (73)	8 (73)	1.0
BMI (g/m <sup>2</sup> )	24.3 ± 2.9	24.2 ± 4.6	0.94
AL-Amyloidosis	7 (64)	–	–
Disease duration (years)	2.19 ± 2.1	–	–
Comorbidities			
Diabetes, n(%)	1 (9)	0 (0)	0.31
Hypertension, n(%)	4 (36)	5 (45)	0.66
CAD, n(%)	0 (0)	0 (0)	1.0
Previous stroke, n(%)	1 (9)	0 (0)	0.31
Class NYHA III-IV n(%)	2 (18)	0 (0)	0.14
Biochemical			
Cholesterol (mmol/L)	5.9 ± 3.2	5.6 ± 1.0	0.794
HDL (mmol/L)	1.3 ± 0.5	1.5 ± 0.4	0.187
Non-HDL (mmol/L)	4.5 ± 3.4	4.0 ± 1.0	0.664
LDL (mmol/L)	2.7 ± 1.2	3.3 ± 0.8	0.234
Triglycerides (mmol/L)	2.5 ± 2.9	1.7 ± 0.9	0.358
NT-proBNP (ng/L)	1287 ± 1304	–	–
Creatinine (µg/dL)	110 ± 33.9	–	–
Treatment			
Stem cell transplantation	4 (36)	–	–
Chemotherapy	7 (64)	–	–
Green tea	3 (27)	–	–

AL amyloid light-chain, BMI body mass index, CAD coronary artery disease, GFR glomerular filtration rate, HDL high density lipoprotein, LDL low density lipoprotein, NYHA New York Heart Association, NT-proBNP N-terminal prohormone of brain natriuretic peptide-levels

show a significant alteration, but GLS and GCS were significantly reduced compared to controls ( $p < 0.001$  for GLS and  $p = 0.007$  for GCS). Circumferential peak longitudinal strain rate as a surrogate for diastolic function was decreased in amyloidosis patients ( $p = 0.019$ ). Fibrosis extent in the amyloidosis patients ranged from 2 to 74% (mean:  $36.1 \pm 27.1\%$ ) of the LV wall.

Apart from an elevated LVEDV (AL vs. ATTR:  $119.4 \pm 20.1$  vs.  $148.8 \pm 14.9$ ,  $p = 0.032$ ) and a trend towards a decrease in GLS and GCS (AL vs. ATTR: GLS =  $-21.9 \pm 4.5$  vs.  $-15.8 \pm 5.7\%$ ,  $p = 0.08$ ; GCS =  $-32.4 \pm 5.4$  vs.  $-25.3 \pm 4.7\%$ ,  $p = 0.058$ ) for the ATTR-type, there was no significant difference between both groups.

At the time of the CMR exam, 4 amyloidosis patients had already received autologous stem cell transplantation. Those patients showed improved GCS and circumferential strain rate in comparisons to the medically treated patients (GCS =  $-34.5 \pm 5.0$  vs.  $-27.2 \pm 5.2\%$ ,

**Table 2** Baseline CMR characteristics of patients and controls

	Amyloidosis	Controls	P-value
LVEF (%)	60.0 ± 13.2	66.1 ± 4.3	0.170
IVS (mm)	18.0 ± 4.6	8.0 ± 1.5	< 0.001
LVMi(g/m <sup>2</sup> )	85.2 ± 25.1	45.0 ± 8.7	< 0.001
LVEDV (mL)	130.1 ± 23.0	126.9 ± 34.0	0.8
LVEDD (mm)	46.2 ± 3.5	46.9 ± 4.6	0.678
SV (mL)	76.7 ± 16.3	84.5 ± 20.2	0.331
RVEF (%)	64.5 ± 9.5	62.8 ± 5.0	0.604
RVEDV (mL)	112.0 ± 30.5	130.1 ± 29.3	0.171
GLS (%)	-19.7 ± 5.6	-31.1 ± 5.5	< 0.001
GCS (%)	-29.8 ± 6.1	-36.2 ± 3.3	0.007
Long SRe	1.7 ± 0.5	1.4 ± 0.4	0.076
Circ SRe	1.3 ± 0.3	1.7 ± 0.4	0.019

Circ circumferential, GLS global longitudinal strain, GCS global circumferential strain, IVS interventricular septum, Long longitudinal, LVEDD left ventricular end-diastolic diameter, LVEDV/RVEDV left/right ventricular end-diastolic volume, LVEF/RVEF left/right ventricular ejection fraction, LVMi left ventricular mass indexed to body surface area, SRe strain rate, SV stroke volume

$p = 0.048$ ; circumferential strain rate =  $1.5 \pm 0.3$  vs.  $1.2 \pm 0.2 \text{ s}^{-1}$ ,  $p = 0.06$ ) with no statistical significance compared to the normal controls.

### Spectroscopy

Spectroscopic data revealed decreased TG/W ratios of  $0.53 \pm 0.23\%$  for the cardiac amyloidosis group in comparison to the control group ( $0.80 \pm 0.26\%$ ,  $p = 0.015$ ) (Figs. 3 & 4). Myocardial CR/W ratios did not show significant differences between both groups, although amyloidosis patients exhibited a larger variation by means of SD (amyloidosis vs controls:  $0.09 \pm 0.08$  vs.  $0.09 \pm 0.03\%$ ). Dividing amyloidosis patients according to their type of amyloidosis or according to their previous treatment (+/- stem cell therapy), no differences in TG/W and CR/W ratios could be detected.

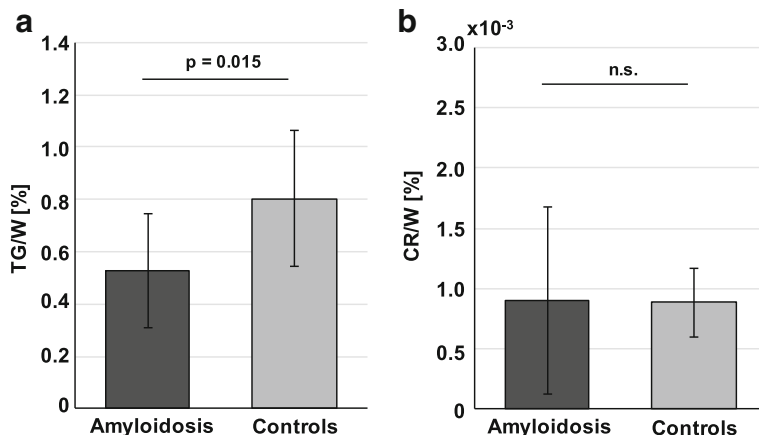
### Correlation analysis

Figure 5 shows bivariate Pearson's correlation between imaging parameters of LV-hypertrophy or function and TG/W ratios. Decreasing TG/W ratios with increasing LVMi and IVS were found (IVS:  $R = -0.46$ ,  $p = 0.033$ ; LVMi:  $R = -0.59$ ,  $p = 0.004$ ).

Comparing myocardial functional LV parameters, there was no correlation between TG/W and LVEF, but there was for TG/W and GLS ( $R = -0.46$ ,  $p = 0.033$ ) and GCS ( $R = -0.48$ ,  $p = 0.025$ ). Fibrosis, age, NT-proBNP and blood lipid levels did not show any correlations. CR/W did not correlate to any of those parameters.

### Discussion

In the present study, CMR spectroscopy identified reduced TG/W ratios, but no change of CR/W in patients



**Fig. 3** Mean and SD of TG/W and CR/W ratios in patients with amyloidosis compared to an age- and BMI-matched normal control group. TG/W, triglyceride-to-water; Cr/W, creatine-to-water; SD, standard deviation

with cardiac amyloidosis when compared to age-matched controls. TG/W was negatively correlated with the severity of LV thickening and LV strain, but not with LVEF.

The reduced myocardial TG/W ratios in the myocardium of patients with amyloidosis are in line with previous studies describing reduced TG content in patients with HCM [8, 11]. Fatty acids (FA) are the major source for myocardial energy in the healthy heart [9, 10]. However myocardial FA oxidation is impaired in heart failure, which in turn, may also trigger myocardial TG accumulation [8, 26, 27]. Recent literature and the

current findings indicate that the pathophysiology of myocardial thickening and/or LVH may play an additional role in myocardial TG accumulation. In HCM, decreasing TG content has been reported [11]. In secondary LVH (e.g. valvular or Anderson-Fabry’s disease) different results can be found depending on the pathogenesis [13, 28]. In mild hypertrophy caused by competitive sports, TG content was preserved [28]. Surprisingly, Anderson-Fabry’s disease that presents with an accumulation of sphingolipids did not associate with an increased TG content [13].

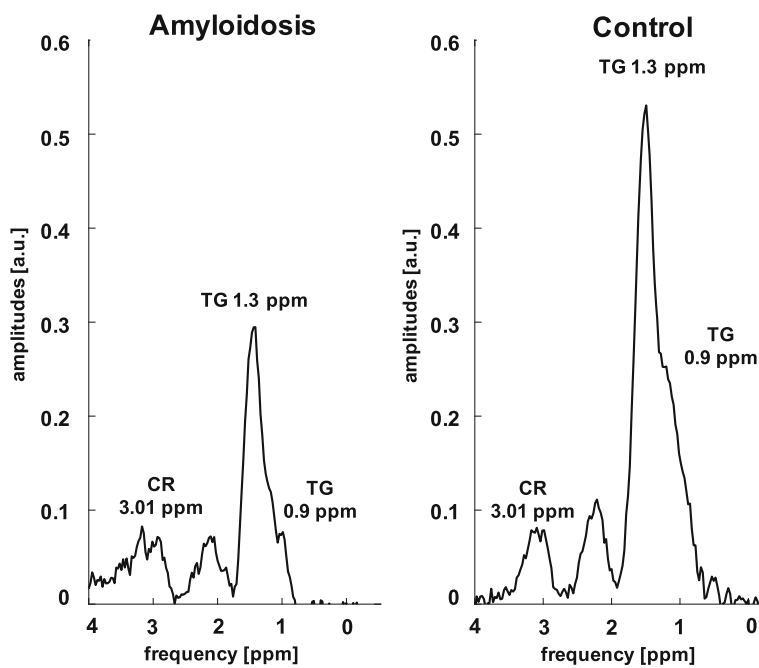
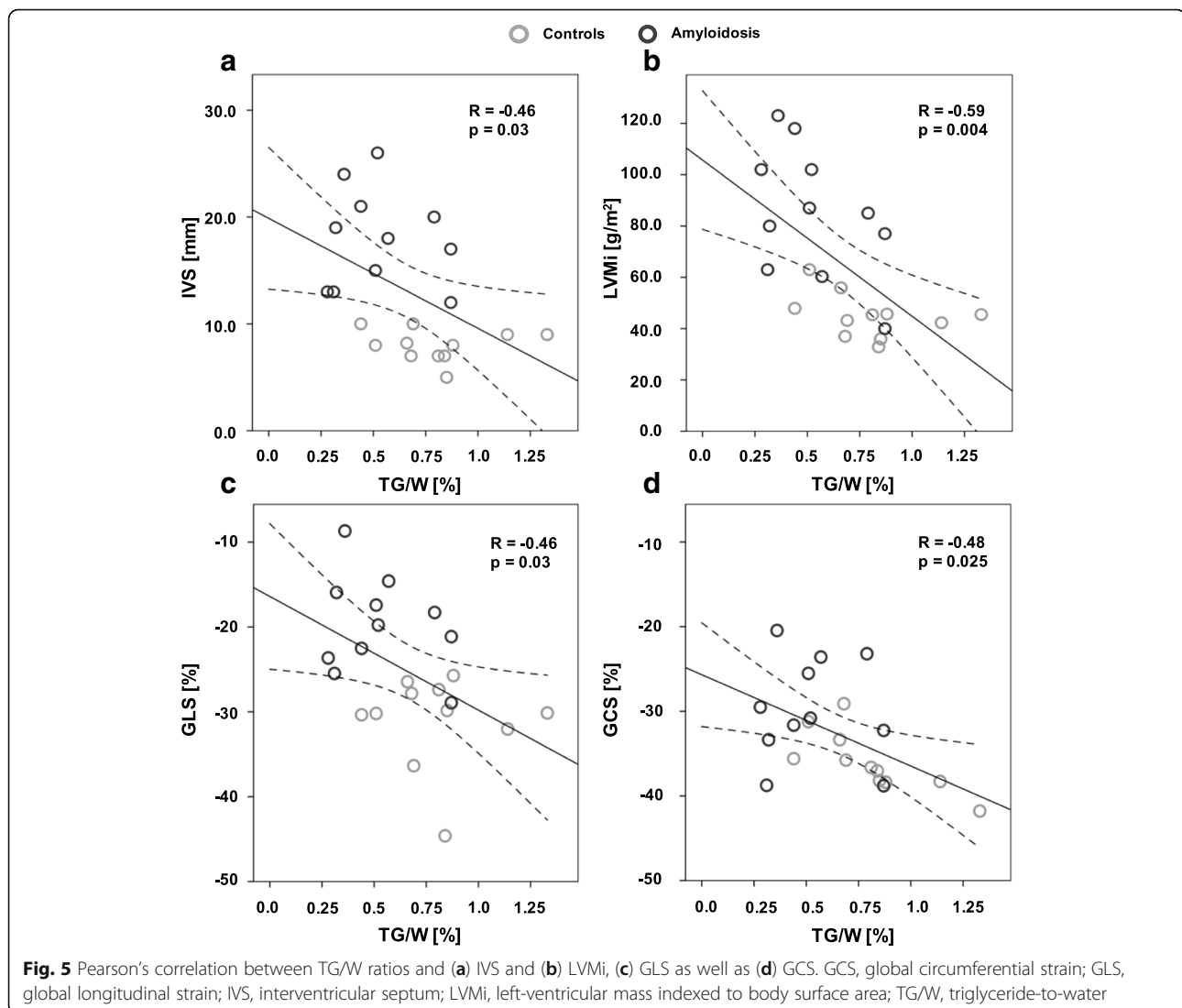


**Fig. 4** Exemplary spectra in a patient with amyloidosis and in a control. TG/W, triglyceride-to-water; CR/W, creatine-to-water; ppm, part per million



In the general context, CMR spectroscopy studies suggest that accumulation of lipids in LVH and heart failure is most pronounced when associated with obesity, overweight or diabetes [29, 30]. Only one subject of the present study suffered from diabetes. Indeed, the person with cardiac amyloidosis suffering from diabetes and additional overweight (body mass index (BMI) > 25 kg/m<sup>2</sup>) exhibited one of the highest TG/W ratios within the amyloidosis cohort. This indicates that these two risk factors might offset the reduction in TG/W ratios. TG/W ratios did not correlate with BMI, blood lipid levels or age in the present study, suggesting that TG/W ratios may associate with other factors, such as the accumulation of amyloid proteins. This is indicated by the negative relationship between TG content and the severity of the thickened myocardium (Fig. 5) and a known histologic correlation of amyloid and the amount of fibrosis [31].

Amyloid proteins of any type mainly deposit within the myocardial interstitium and extend the extracellular volume which may hamper extramyocellular TG deposition [32, 33]. So far, the direct influence of amyloid on TG is unknown, but an increasing effect on the T<sub>1</sub>-values of the global myocardium has already been described [3]. As a consequence of the prolonged T<sub>1</sub>-values of tissue water, partial saturation increases using PRESS with a fixed TR of 2000 ms. Correcting the water signal for those T<sub>1</sub>-values would increase the signal by approximately 10% and therefore the TG/W ratio would further decrease below the value stated above. Another possible mechanism may relate to the myocytotoxic effects of circulating amyloid light chains and their influence on mitochondrial function, i.e. the β-oxidation of free fatty acids [34–36]. This interaction causes oxidative stress of the cell leading to the toxic effects in proteins, lipids, DNA and inflammatory processes [27]. Not only amyloid



light chains interact with free FAs, but also the amyloid of Alzheimer's disease that reduces unsaturated fatty acids in certain parts of the brain known to cause dementia [37]. However, further research of the exact mechanism of metabolic alterations in cardiac amyloidosis has to be pursued.

Results in the age-matched controls were in line with previous literature [38, 39]. To address diurnal changes of TG/W, subjects and patients were scanned during afternoon hours and with a prior fasting period of about 3 h [40].

No mean difference of CR/W could be detected between patients and controls. However, SD of myocardial CR was higher in the amyloidosis group potentially due to different disease states of the patients [41, 42]. In contrast to previous studies, no correlation between CR/W ratios and LV function parameters could be detected [10, 43]. It should, however, be noted that fitting of CR peaks is challenging due to their low signal and hence results may be confounded by fitting errors [9].

Although  $^1\text{H}$ -CMRS has not yet found its way into clinical routine due to technical demands and the still time-consuming scan,  $^1\text{H}$ -CMRS may add clinical value by detecting metabolic changes in the course of developing cardiac amyloidosis. Considering the current progress regarding scan time reduction and ease-of-use of  $^1\text{H}$ -CMRS, there is the potential to integrate the method into standard imaging workflows.

Besides LGE, parametric imaging techniques including  $T_1$  and extracellular volume (ECV) mapping have been used in cardiac amyloidosis to distinguish different amyloidosis types [44, 45]. Both LGE and ECV mapping require gadolinium injection which excludes patients with severe renal insufficiency. In these patients, expansion of ECV may be identified through changes in the triglyceride levels using  $^1\text{H}$ -CMRS. Moreover, modulation of TG/W values may point directly to myocytotoxic effects of circulating amyloid chains which potentially contribute to ECV expansion as measured with  $T_1$ /ECV mapping [27]. These insights, however, remain to be established through larger studies in the future.

### Limitations

The present sample size was relatively small due to the technical demands of the study. Subject numbers were however comparable to previous studies assessing myocardial metabolism in heart failure [11, 28]. Assuming decreased myocardial TG/W according to literature, we sought to identify an effect in comparison to normal controls with a statistical power of 90% and type I error of less than 5%, resulting in an estimated sample size of 10 per group [11].

As cardiac amyloidosis had already been confirmed in all patients at the time of CMR, we did not perform

myocardial biopsies to quantify myocardial TG content and to differentiate intramyocellular (IMCL) and extramyocellular lipids (EMCL). The differentiation of IMCL and EMCL may help to understand the mechanism of the TG/W reduction in cardiac amyloidosis and whether it is caused by expanded extracellular space or by a reduced metabolism of myocytes. Although recent work has shown feasibility to quantify IMCL and EMCL in the human heart using spectroscopy, the present method could not reliably differentiate between the different pools [46].

### Conclusions

Myocardial TG/W decreases in cardiac amyloidosis and is associated with the severity of myocardial thickening and systolic dysfunction, independent of age, BMI and blood lipid levels. CMR proton spectroscopy may provide additional information to gauge progression of cardiac amyloidosis.

### Abbreviations

$^1\text{H}$ -CMRS: Cardiac proton magnetic resonance spectroscopy; AL: Light-chain amyloidosis; AS: Aortic stenosis; ATTR: Transthyretin-related amyloidosis; BMI: Body mass index; bSSFP: balanced steady-state free precession; CAD: Coronary artery disease; CHESS: Chemical shift selective saturation; CMR: Cardiovascular magnetic resonance; CR: Creatine; CR/W: Creatine-to-water ratio; ECG: Electrocardiogram; ECV: Extracellular volume; eGFR: Estimated glomerular filtration rate; EMCL: Extramyocellular lipids; FA: Fatty acids; FWHM: Full width at half maximum; GCS: Global circumferential strain; GLS: Global longitudinal strain; HCM: Hypertrophic cardiomyopathy; HDL: High density lipoprotein; HLSVD: Hankel-Lanczos Singular Value Decomposition; IMCL: intramyocellular lipids; IVS: Interventricular septum; LDL: Low density lipoprotein; LGE: Late gadolinium enhancement; LVEDV: Left ventricular end-diastolic volume; LVEF: Left ventricular ejection fraction; LVH: Left ventricular hypertrophy; LVM(i): Left ventricular indexed mass; NT-proBNP: N-terminal prohormone of brain natriuretic peptide; NYHA: New York Heart Association; PRESS: Point-resolved spectroscopy; RVEDV: Right ventricular end-diastolic volume; RVEF: Right-ventricular ejection fraction; SD: Standard deviation; SRe: Strain rate; SV: Stroke volume; SVD: Singular value decomposition; TE: Echo time; TG: Triglyceride; TG/W: Triglyceride-to-water ratio; TMA: Trimethylammonium; TR: Repetition time; VOI: Volume of interest

### Funding

German research Foundation, Research Fellowship to Mareike Gastl (GA 2621/1–1).

### Availability of data and materials

The datasets used and analyzed during the current study are available from the corresponding author on reasonable request.

### Authors' contributions

MG, SP and SK conceived the study design. MG, SP, AG and CvD obtained CMR images. MG and SP analyzed CMR scans and the data. MG drafted the manuscript. SP, AG, MF, CvD, FB, MK, AF, RS, RM and SK critically revised the manuscript. All authors substantially contributed and approved the final manuscript.

### Ethics approval and consent to participate

The study design was approved by the local ethics committee (Kantonale Ethikkommission Zürich) and was conducted according to the Declaration of Helsinki.

### Consent for publication

Written informed consent was obtained from all study participants.

**Competing interests**

All authors declare no competing interests.

**Publisher's Note**

Springer Nature remains neutral with regard to jurisdictional claims in published maps and institutional affiliations.

**Author details**

<sup>1</sup>Institute for Biomedical Engineering, University and ETH Zurich, Gloriastrasse 35, 8092 Zurich, Switzerland. <sup>2</sup>Department of Cardiology, University Heart Center, University Hospital Zurich, Zurich, Switzerland. <sup>3</sup>Department Cardiology, Pneumology and Angiology, Heinrich Heine University, Düsseldorf, Germany. <sup>4</sup>Comprehensive Cancer Center Zürich, University Hospital Zurich, Zurich, Switzerland. <sup>5</sup>Institute of Diagnostic and Interventional Radiology, University Hospital Zurich, Zurich, Switzerland.

Received: 15 October 2018 Accepted: 4 January 2019

Published online: 31 January 2019

**References**

- vanden Driesen RI, Slaughter RE, Strugnell WE. MR findings in Cardiac Amyloidosis. *Am J Roentgenol*. 2006;186:1682–5.
- Quarta CC, Kruger JL, Falk RH. Cardiac Amyloidosis. *Circulation*. 2012;126:e178–82.
- Banyersad SM, Fontana M, Maestrini V, Sado DM, Captur G, Petrie A, et al. T1 mapping and survival in systemic light-chain amyloidosis. *Eur Heart J*. 2015;36:244–51.
- Falk RH. Diagnosis and management of the cardiac amyloidoses. *Circulation*. 2005;112:2047–60.
- Gillmore JD, Maurer MS, Falk RH, Merlini G, Damy T, Dispenzieri A, et al. Nonbiopsy diagnosis of Cardiac transthyretin Amyloidosis. *Circulation*. 2016;133:2404–12.
- Dungu JN, Valencia O, Pinney JH, Gibbs SDJ, Rowczenio D, Gilbertson JA, et al. CMR-based differentiation of AL and ATTR Cardiac Amyloidosis. *JACC Cardiovasc Imaging*. 2014;7:133–42.
- Martinez-Naharro A, Treibel TA, Abdel-Gadir A, Bulluck H, Zumbo G, Knight DS, et al. Magnetic resonance in transthyretin Cardiac Amyloidosis. *J Am Coll Cardiol*. 2017;70:466–77.
- Neubauer S. The failing heart — An engine out of fuel. *N Engl J Med*. 2007;356:1140–51.
- van Ewijk PA, Schrauwen-Hinderling VB, Bekkers SCAM, Glatz JFC, Wildberger JE, Kooi ME. MRS: a noninvasive window into cardiac metabolism. *NMR Biomed*. 2015;28:747–66.
- Faller KME, Lygate CA, Neubauer S, Schneider JE. 1H-MR spectroscopy for analysis of cardiac lipid and creatine metabolism. *Heart Fail Rev*. 2012;18:657–68.
- Nakae I, Mitsunami K, Yoshino T, Omura T, Tsutamoto T, Matsumoto T, et al. Clinical features of myocardial triglyceride in different types of cardiomyopathy assessed by proton magnetic resonance spectroscopy: comparison with myocardial creatine. *J Card Fail*. 2010;16:812–22.
- Mahmod M, Bull S, Suttie JJ, Pal N, Holloway C, Dass S, et al. Myocardial steatosis and left ventricular contractile dysfunction in patients with severe aortic stenosis. *Circ Cardiovasc Imaging*. 2013;6:808–16.
- Petritsch B, Köstler H, Weng AM, Horn M, Gassenmaier T, Kunz AS, et al. Myocardial lipid content in Fabry disease: a combined 1H-MR spectroscopy and MR imaging study at 3 tesla. *BMC Cardiovasc Disord*. 2016;16:205.
- Ami D, Lavatelli F, Rognoni P, Palladini G, Raimondi S, Giorgetti S, et al. In situ characterization of protein aggregates in human tissues affected by light chain amyloidosis: a FTIR microspectroscopy study. *Sci Rep*. 2016;6:29096.
- Miyahara H, Sawashita J, Ishikawa E, Yang M, Ding X, Liu Y, et al. Comprehensive proteomic profiles of mouse AApoAll amyloid fibrils provide insights into the involvement of lipoproteins in the pathology of amyloidosis. *J Proteome*. 2017;172:111–21.
- Gertz MA, Comenzo R, Falk RH, Fermand JP, Hazenberg BP, Hawkins PN, et al. Definition of organ involvement and treatment response in immunoglobulin light chain amyloidosis (AL): a consensus opinion from the 10th international symposium on amyloid and Amyloidosis. *Am J Hematol*. 2005;79:319–28.
- Morsbach F, Gordic S, Gruner C, Niemann M, Goetti R, Gotschy A, et al. Quantitative comparison of 2D and 3D late gadolinium enhancement MR imaging in patients with Fabry disease and hypertrophic cardiomyopathy. *Int J Cardiol*. 2016;217:167–73.
- Weiss K, Summermatter S, Stoeck CT, Kozerke S. Compensation of signal loss due to cardiac motion in point-resolved spectroscopy of the heart. *Magn Reson Med*. 2014;72:1201–7.
- Haase A, Frahm J, Hänicke W, Matthaei D. 1H NMR chemical shift selective (CHESS) imaging. *Phys Med Biol*. 1985;30:341–4.
- Weiss K, Martini N, Boesiger P, Kozerke S. Cardiac proton spectroscopy using large coil arrays. *NMR Biomed*. 2013;26:276–84.
- Fuetterer M, Stoeck CT, Kozerke S. Second-order motion compensated PRESS for cardiac spectroscopy. *Magn Reson Med*. 2017;77:57–64.
- Naresi A, Couturier C, Devos JM, Janssen M, Mangeat C, de Beer R, et al. Java-based graphical user interface for the MRUI quantitation package. *MAGMA*. 2001;12:141–52.
- Nakae I, Mitsunami K, Matsuo S, Matsumoto T, Morikawa S, Inubushi T, et al. Assessment of myocardial creatine concentration in dysfunctional human heart by proton magnetic resonance spectroscopy. *Magn Reson Med Sci*. 2004;3:19–25.
- Amado LC, Gerber BL, Gupta SN, Rettmann DW, Szarf G, Schock R, et al. Accurate and objective infarct sizing by contrast-enhanced magnetic resonance imaging in a canine myocardial infarction model. *J Am Coll Cardiol*. 2004;44:2383–9.
- Ponikowski P, Voors AA, Anker SD, Bueno H, Cleland JGF, Coats AJS, et al. 2016 ESC guidelines for the diagnosis and treatment of acute and chronic heart failure. *Eur J Heart Fail*. 2016;18:891–975.
- Osorio JC, Stanley WC, Linke A, Castellari M, Diep QN, Panchal AR, et al. Impaired myocardial fatty acid oxidation and reduced protein expression of retinoid X receptor-alpha in pacing-induced heart failure. *Circulation*. 2002;106:606–12.
- Doenst T, Nguyen TD, Abel ED. Cardiac metabolism in heart failure: implications beyond ATP production. *Circ Res*. 2013;113:709–24.
- Secchi F, Di Leo G, Petrini M, Spairani R, Ali M, Guazzi M, et al. 1H- and 31P-myocardial magnetic resonance spectroscopy in non-obstructive hypertrophic cardiomyopathy patients and competitive athletes. *Radiol Med*. 2017;122:265–72.
- Sharma S, Adrogue JV, Golfman L, Uray I, Lemm J, Youker K, et al. Intramyocardial lipid accumulation in the failing human heart resembles the lipotoxic rat heart. *FASEB J*. 2004;18:1692–700.
- Szczepaniak LS, Dobbins RL, Metzger GJ, Sartoni-D'Ambrosia G, Arbiq D, Vongpatanasin W, et al. Myocardial triglycerides and systolic function in humans: in vivo evaluation by localized proton spectroscopy and cardiac imaging. *Magn Reson Med*. 2003;49:417–23.
- Mohammed SF, Mirzoyev SA, Edwards WD, Dogan A, Grogan DR, Dunlay SM, et al. Left ventricular amyloid deposition in patients with heart failure and preserved ejection fraction. *JACC Heart Fail*. 2014;2:113–22.
- Maleszewski JJ. Cardiac amyloidosis: pathology, nomenclature, and typing. *Cardiovasc Pathol*. 2015;24:343–50.
- Haaf P, Garg P, Messroghli DR, Broadbent DA, Greenwood JP, Plein S. Cardiac T1 mapping and extracellular volume (ECV) in clinical practice: a comprehensive review. *J Cardiovasc Magn Reson*. 2017;18:89.
- Liao R, Jain M, Teller P, Connors LH, Ngoy S, Skinner M, et al. Infusion of light chains from patients with cardiac amyloidosis causes diastolic dysfunction in isolated mouse hearts. *Circulation*. 2001;104:1594–7.
- Brenner DA, Jain M, Pimentel DR, Wang B, Connors LH, Skinner M, et al. Human Amyloidogenic light chains directly impair cardiomyocyte function through an increase in cellular oxidant stress. *Circ Res*. 2004;94:1008–10.
- Lavatelli F, Imperlini E, Orrù S, Rognoni P, Sarnataro D, Palladini G, et al. Novel mitochondrial protein interactors of immunoglobulin light chains causing heart amyloidosis. *FASEB J*. 2015;29:4614–28.
- Snowden SG, Ebshtiana AA, Hye A, An Y, Pletnikova O, O'Brien R, et al. Association between fatty acid metabolism in the brain and Alzheimer disease neuropathology and cognitive performance: a nontargeted metabolomic study. *PLoS Med*. 2017;14:e1002266.
- Petritsch B, Gassenmaier T, Kunz A, Donhauser J, Goltz J, Bley T, et al. Age dependency of myocardial triglyceride content: a 3T high-field 1H-MR spectroscopy study. *RöFo*. 2015;187:1016–21.
- van der Meer RW, Rijzewijk LJ, Diamant M, Hammer S, Schär M, Bax JJ, et al. The ageing male heart: myocardial triglyceride content as independent predictor of diastolic function. *Eur Heart J*. 2008;29:1516–22.
- Ith M, Stettler C, Xu J, Boesch C, Kreis R. Cardiac lipid levels show diurnal changes and long-term variations in healthy human subjects. *NMR Biomed*. 2014;27:1285–92.

41. Rapezzi C, Perugini E, Salvi F, Grigioni F, Riva L, Cooke RMT, et al. Phenotypic and genotypic heterogeneity in transthyretin-related cardiac amyloidosis: towards tailoring of therapeutic strategies? *Amyloid*. 2006;13:143–53.
42. Fikrle M, Paleček T, Kuchynka P, Němeček E, Bauerová L, Straub J, et al. Cardiac amyloidosis: a comprehensive review. *Cor Vasa*. 2013;55:e60–75.
43. Nakae I, Mitsunami K, Matsuo S, Horie M. Creatine depletion and altered fatty acid metabolism in diseased human hearts: clinical investigation using  $^1\text{H}$  magnetic resonance spectroscopy and  $^{123}\text{I}$  BMIPP myocardial scintigraphy. *Acta Radiol*. 2007;48:436–43.
44. Karamitsos TD, Piechnik SK, Banyersad SM, Fontana M, Ntusi NB, Ferreira VM, et al. Noncontrast T1 mapping for the diagnosis of Cardiac Amyloidosis. *JACC Cardiovasc Imaging*. 2013;6:488–97.
45. Fontana M, Banyersad SM, Treibel TA, Abdel-Gadir A, Maestrini V, Lane T, et al. Differential myocyte responses in patients with Cardiac transthyretin Amyloidosis and light-chain Amyloidosis: a Cardiac MR imaging study. *Radiology*. 2015;277:388–97.
46. Fillmer A, Hock A, Cameron D, Henning A. Non-water-suppressed  $^1\text{H}$  MR spectroscopy with Orientational prior knowledge shows potential for separating intra- and Extramyocellular lipid signals in human myocardium. *Sci Rep*. 2017;7:16898.

**Ready to submit your research? Choose BMC and benefit from:**

- fast, convenient online submission
- thorough peer review by experienced researchers in your field
- rapid publication on acceptance
- support for research data, including large and complex data types
- gold Open Access which fosters wider collaboration and increased citations
- maximum visibility for your research: over 100M website views per year

**At BMC, research is always in progress.**

Learn more [biomedcentral.com/submissions](https://biomedcentral.com/submissions)

